Available online at www.sciencedirect.com
ScienceDirect
Advances in Water Resources 29 (2006) 1665–1677
Advances in Water Resources
www.elsevier.com/locate/advwatres

Simulating the value of El Niño forecasts for the Panama Canal

Nicholas E. Graham [a], Konstantine P. Georgakakos [a,*], Carlos Vargas [b], Modesto Echevers [b]

[a] *Hydrologic Research Center, 12780 High Bluff Drive, # 250, San Diego, CA 92130, USA*
[b] *Meteorology and Hydrographic Branch, Engineering Division, Panama Canal Authority, Corozal, Panama*

Received 3 July 2005; received in revised form 14 December 2005; accepted 16 December 2005
Available online 7 February 2006

Abstract

The Panama Canal relies on rain-fed streamflow into Gatun Lake, the canal's primary storage facility, for operations—principally ship passage and hydropower generation. Precipitation in much of Panama has a strong negative relationship with eastern tropical Pacific sea surface temperature (SST) and this relationship is reflected in Gatun Lake inflows. For example, the correlation coefficient between wet season (July–December) inflow and NINO3 SST is −0.53 over the period 1914–1997. Operational capabilities to predict tropical Pacific SSTs have been demonstrated by several forecast systems during the past decade, and (as we show) such SST forecasts can be used to reduce the uncertainty of estimates of future inflows (compared with climatological expectations). Because substantial reductions in lake inflow negatively impact canal operations, we wondered whether these forecasts of future inflows, coupled with a method for translating that information into effective operational policy, might result in more efficient canal management. A combined simulation/optimization/assessment "virtual" canal system was implemented and exercised using operational El Niño forecasts over the period 1981–1998. The results show the following main points:

(i) At current demand levels, the canal system is relatively robust (insensitive to flow forecasts) unless flows are substantially reduced (i.e., during El Niño episodes) or forecasts are extremely accurate.
(ii) The inclusion of accurately specified levels of forecast uncertainty is critical in developing economically beneficial policies.
(iii) The situations in which imperfect forecast information can be useful lie between those where storage and future inflows are relatively high, and those where storage and inflows are relatively low. In the former case, demands can be met without the benefit of forecast information, and in the latter case even perfect forecast information cannot prevent operational curtailments.
(iv) For a nominally configured canal system, the use of operational El Niño forecasts with appropriately specified uncertainty resulted in approximately $US 20,000,000 (about 3%) in increased annual average income compared with the use of deterministic climatological forecasts.

Keywords: El Niño forecasts; Panama Canal management; Forecast uncertainty; Seasonal forecasting; Management under uncertainty

1. Introduction

The Panama Canal is a fresh water, gravity fed canal whose purpose and income derive principally from the passage of vessels; hydroelectric power generation provides a secondary source of income. Canal income contributes importantly to Panama's economy—for example, total revenue in 2003 was $US 921 million [12], or approximately 7% of 2003 gross domestic product [17]. Efficient operation of the canal is not only important at the margins. Major disruptions of canal operations would result in substantial and immediate national economic loss, and shipping interests might then seek alternative means and routes of con-

* Corresponding author. Tel.: +1 858 794 2726; fax: +1 858 792 2519.
E-mail address: KGeorgakakos@hrc-lab.org (K.P. Georgakakos).

0309-1708/$ - see front matter © 2005 Elsevier Ltd. All rights reserved.
doi:10.1016/j.advwatres.2005.12.005

veyance, leading to the loss of future income as well. Of course, in the larger context of global commerce and geopolitics, the Canal is a vital transport link, and any curtailment (or increase) in its ability to pass ships would have far reaching repercussions.

The primary reservoir for the Canal system is Gatun Lake which is fed by a number of rivers and streams, the largest of which (Rio Charges) flows into smaller Madden Lake, which provides managed discharge into Gatun Lake. Thus, Canal water supply and operations are dependent on precipitation. This dependence is strict—at capacity Gatun Lake only holds water sufficient for a few months of self-sustained operations, and inflow itself has a strong annual cycle, with dry season flows an order of magnitude less than those in the wet season. A further element in the hydrologic setting of the Canal is that regional precipitation (and streamflow) is strongly modulated by changes in tropical Pacific sea surface temperatures (SST), most notably those associated with the El Niño/Southern Oscillation (ENSO; [2,15]). This association is strong; for example, water-year rainfall was below average in 11 of 12 El Niño events between 1930 and 1983 (e.g., [3]) and Gatun Lake wet season inflow was below median in 17 of 20 cases in cases when the SST anomaly in the NINO3 region (150–90° W and 5° N–5° S; 1914–1999) was greater than 0.6 C. While the Canal system can withstand most instances of economic variability, major reductions in hydroelectric generation and minor draft restrictions were implemented during the very strong 1982–1983 El Niño episode, and much more substantial enforcements were required during the stronger 1997–1998 event [1].

As described in [1], the availability of qualitative forecast information during the onset and evolution of the 1997–1998 event did have some value with regard to operational planning. The work described here develops the potential utility of seasonal-to-interannual forecasts of tropical Pacific SSTs in a more rigorous framework in which operational SST forecasts are converted to quantitative monthly ensemble inflow forecasts at lead times out to six months. These ensemble inflow forecasts serve as input to a simulation model of Canal storage and operations. This system is exercised by a simulated decision support system that derives economically optimal release policies over the six month planning horizon. The system is updated monthly by application of the observed flows with the optimal policy for one month. The effectiveness of a given forecast system is assessed by summing the income accrued in these assessment steps. Different simulations explored that effectiveness of perfect forecasts, forecasts based on long-term climatology, and others based on operational forecasts of NINO3 SST over the period 1981–1998 [6,7]; each was applied with varying degrees of uncertainty, and using various levels of demand. The results show that accurate forecast information can be of substantial value for Canal planning and economics, and emphasize the importance of accurate specification of uncertainty. This latter result is in line with earlier results in [4] obtained for managed water systems in the extratropics.

Following this introduction the presentation is organized as follows: data and methodology are described in Section 2, Section 3 presents the results, and Section 4 provides a brief summary.

2. Background and methods

2.1. Canal characteristics

The Panama Canal is a gravity-fed, fresh water system for which Gatun Lake acts as the primary control reservoir (see Fig. 1). Gatun Lake is supplied directly by precipitation into the lake, by inflow from three rivers, and by inflow from Lake Madden, which is also fed by three rivers. The useful volume (V^*) of Gatun Lake is 766 Mm^3 (10^6 m^3), residing between a maximum (spill) level of 26.6 m and a minimum useful level of 24.8 m (below which ship traffic cannot be maintained). Average monthly inflow varies from 82 to 860 Mm^3 per month. The available supply is used for principally two purposes: lockage (ship traffic) and hydroelectric generation. The canal can pass (nominally) 40 ships per day, with each ship transit requiring approximately 197,000 m^3, so one month of full lockage operations requires 236.2 Mm^3, or approximately 30% of useful lake volume at capacity. For our simulations, a nominal canal-income value of $US 50,000 was used for each ship transit, and the canal (as simulated) can earn $US 60M per month through lockage alone.

Gatun Lake has 24 MW of installed hydropower generation capacity; one month of full capacity hydroelectric generation would require 330 Mm^3 of water. Water used for hydroelectric generation is not available for lockage. For our simulations, the power price was set at $US 50 per MW h (mega-watt hour), for a maximum possible monthly income of $US 864,000. Thus, 10^6 cubic meters of water used for simulated lockage generates about $US 254,000 of income, while that same amount of water used for simulated hydroelectric generation produces $US 2618.

Spillage for Gatun Lake is managed through a set of 14 gates, through which water can be passed at a (total) maximum rate of 445.28 Mm^3 per day (due to downstream impacts, this rate is rarely reached). High spillage rates result in curtailments of hydropower generation; this effect is not included in the simulation. Spillage operations are episodic and typically less than 10 days running. Further discussion of the handling of simulated spilling is given in Section 2.3.2. For this study, simulated evaporation losses were parameterized as 6.2 Mm^3 per month (74 Mm^3 annually). The canal supplies a similar amount of water for municipal use; this amount was not accounted for in the simulations.

Giving priority to nominal lockage (down to levels near the minimum useful level), Gatun Lake level is managed using a rule curve that gives target levels for each day of

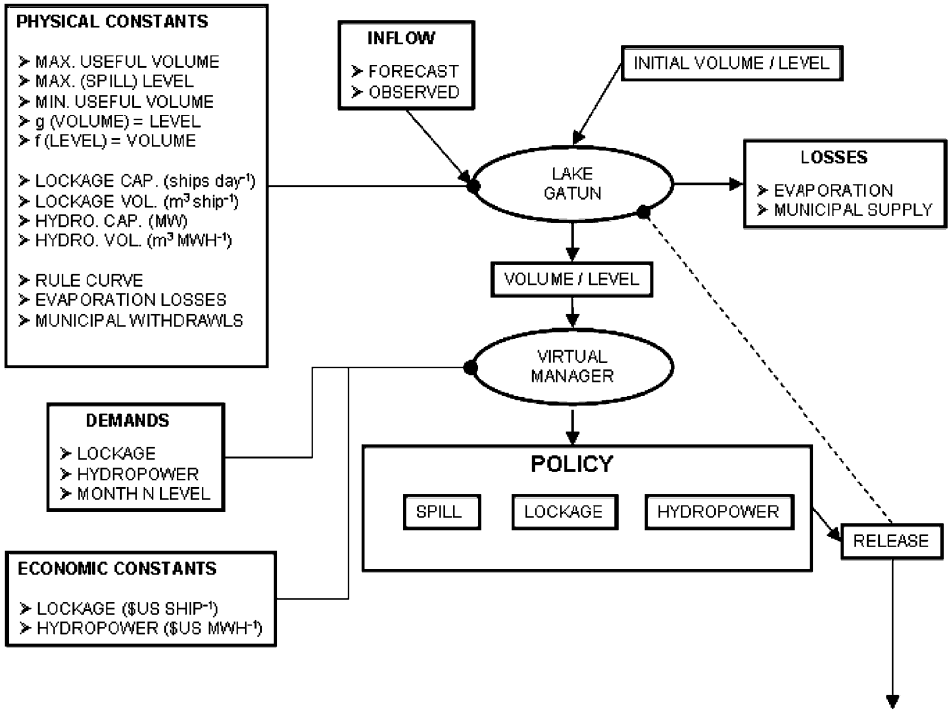

Fig. 1. Schematic of the simulated Panama Canal system.

the year. The rule curve is based on the annual cycle of inflow, canal storage and conveyance capacities, and operational goals. The basic rationale is to fill Gatun Lake to near capacity by the end of the wet season (avoiding excessive spillage), and draw it down slowly during the dry season.

2.2. Climatology

Fig. 2 shows the annual cycle of median (p50) Gatun Lake inflow (1950–1999) with the corresponding 20th (p20) and 80th (p80) percentile bounds. Inflow has a strong annual cycle with the minimum (median) occurring in March (82 Mm^3) and the maximum in November (860 Mm^3). The variability of the monthly flow (p80 − p20) is only weakly related to median flow, but as can be appreciated from Fig. 2, the relative variability range ((p80 − p20)/p50), not shown) tends to be higher during the dry season (typically > 0.75; maximum 1.43 in April) than during the wet season (values typically <0.60; minimum 0.32 in September); relative variability in December is anomalously high (1.0) in comparison to the relative high median inflow.

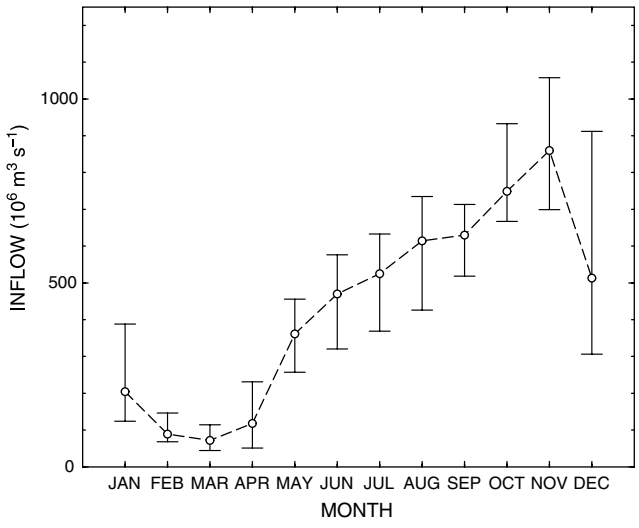

Fig. 2. Annual cycle of median Gatun Lake inflow for 1950–1999. Error bars give the 20th and 30th percentiles.

As noted in the Introduction, precipitation and streamflow in the Panama Canal region (and much of Central America in general) is strongly modulated by tropical Pacific sea surface temperatures. For example, Fig. 3 shows correlations between water year (April–March, 1915–1999) Gatun Lake inflow and tropical SSTs (from the data set of Smith and Reynolds [16, cf. 14]). The negative association between inflow and eastern tropical Pacific SSTs is clear, with widespread values between −0.4 and −0.5.

A scatter plot (Fig. 4) of wet season (July–December) Gatun Lake inflow and NINO3 SST anomaly [area-average for 150° W to 90° W, 5° S to 5° N; Smith and Reynolds [16] data] shows an approximately linear relationship with an overall correlation coefficient of 0.56. The point plotted at the extreme lower right in Fig. 4 represents the low flows experienced during the strong 1997–1998 El Niño episode; the point with the highest inflows represents July–December 1936.

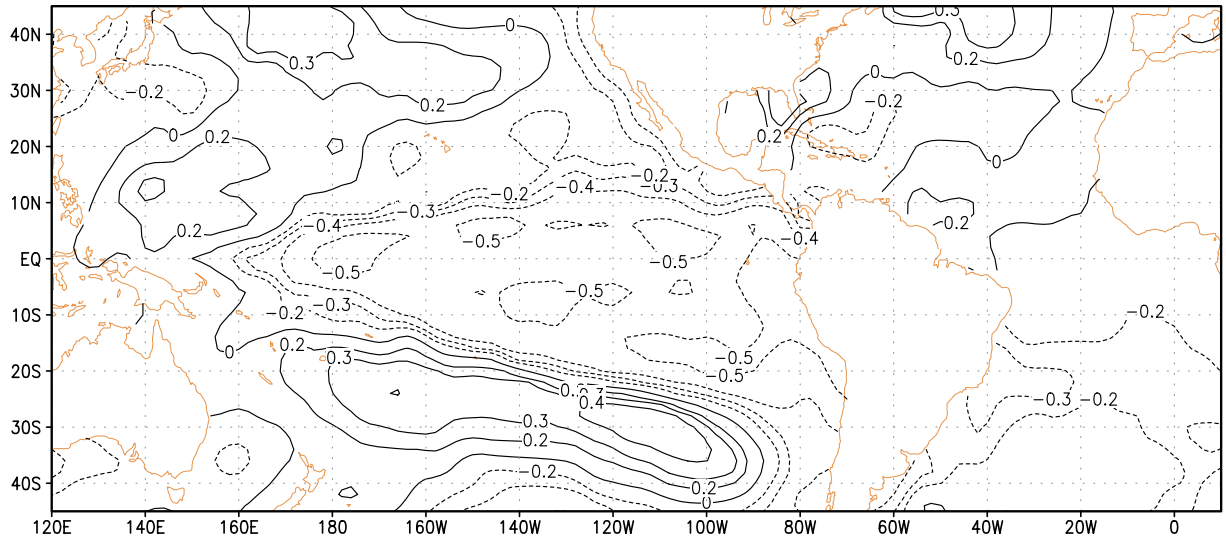

Fig. 3. Correlations for April–March average SST and Gatun Lake inflow; analysis for 1914–1915 to 1998–1999.

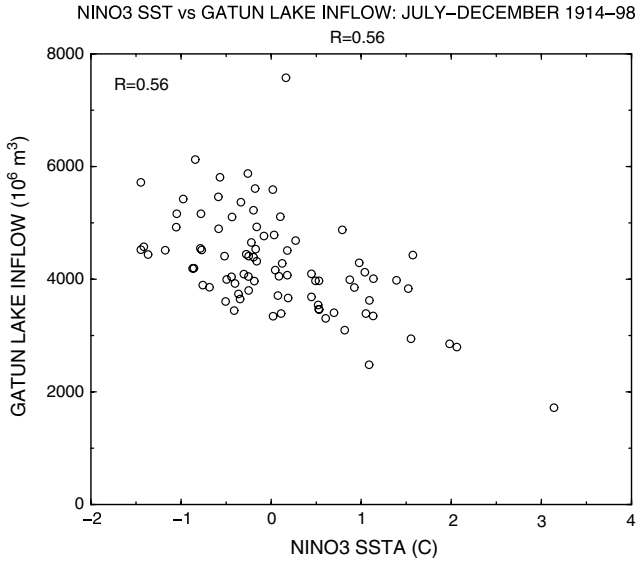

Fig. 4. Scatter plot of July–December average NINO3 SST anomaly (horizontal axis) and Gatun Lake inflow (vertical axis); data for 1914–1998.

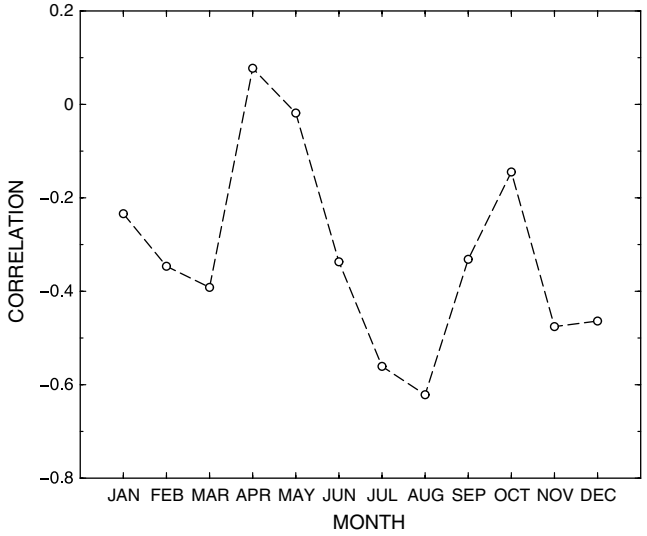

Fig. 5. Annual cycle of correlations between Gatun Lake inflow and NINO3 SST (1950–1999).

The annual cycle of correlations (Fig. 5) between Gatun Lake inflow and NINO3 SST (1950–1999) shows a complex pattern, with correlations ranging from −0.35 to −0.5 in November, December, February, and March, and from June through September. The closest relationships occur in July–August (correlations near −0.6) and November–December (correlations near −0.5), during the early and late phases on the wet season. October (climatologically the second wettest month of the year) is notable for having very little systematic relationship with tropical Pacific SSTs suggesting that ITCZ-related rainfall tends to reach Panama during this month whatever the modulating effects from the tropical Pacific. Why the relationship between inflow and NINO3 SST is so much in stronger in November than in October has not been investigated, but the effect is clear in comparison of scatter plots (not shown), and results primarily (but not solely) from a strong positive inflow response in years with cool NINO3 SSTs in November (behavior that substantially increases the November average). In comparison, the corresponding scatter plot for October inflow indicates little systematic relationship linear or otherwise.

2.3. Simulation, optimization, and assessment

2.3.1. The problem

The basic problem approached here is to derive an optimal release policy (i.e., for lockage, hydropower, and spill) for canal operations through an M-month forecast horizon given the following information:

(A) An ensemble of inflow forecasts (Q_F), in this case generated using inflow forecasts with a defined uncertainty distribution,
(B) The initial state of Gatun Lake (for this work, the initial volume (V_0), or equivalently, the initial level (H_0)).
(C) Operational specifications:
- Water volumes (releases) required for ship passage (lockage; R_L, m^3 $ship^{-1}$) and hydropower generation (R_H, m^3 MW h^{-1}).
- Maximum (spill) and minimum (useful) volume and level (V^U, V^L (m^3); H^U, H^L (m)).
- Maximum possible release rates through lockage (R_L^U), hydropower generation (R_H^U), and spill (R_S^U); all m^3 $month^{-1}$.
- Uncontrolled loss rates (municipal withdrawals and evaporation, cast here as a volumetric constant, E (m^3 $month^{-1}$)).
- Functions $g(V)$, and its inverse $h(H)$, relating lake volume to lake level, and lake level to lake volume, respectively.

(D) Economic specifications:
- Lockage income (i_L, \$US $ship^{-1}$).
- Hydropower generation income (i_H, \$US MW h^{-1}).

(E) An objective function (J) quantifying the operational goals. For this work, J is stated in terms of functions relating to (i) total income (I) through the forecast horizon, and (ii) the departure of canal level from the rule curve (H_m^*, see Section 2.1) at the end of the forecast horizon.

The optimal policy is stated as a set of M releases for lockage, hydropower, and spill (R_{Lj},R_{Hj},R_{Sj}) through the forecast horizon (i.e., $1 < j < M$). Unless required, the temporal subscript (j) is dropped in the rest of the discussion. Also note that the product $R_L^U V_L^{-1}$ (which appears in several places) simply expresses the maximum monthly lockage in terms of ships rather than as a water volume. Similarly, the product $R_H^U V_H^{-1}$, gives the maximum possible monthly hydroelectric generation in terms of MW h.

More formally, the problem is to obtain R that minimizes the ensemble-wide expectation of the objective function through the forecast horizon,

$$\langle J \rangle = F(I) + G(\delta H_{FIN}), \tag{1}$$

subject to canal initial state (V_0), inflow forecast ensemble (or distribution) (Q_F), and relevant physical and economic constraints, where

$$F(I) = 1 - [(I_L + I_H)/I_{max}], \tag{2}$$

with

$$I_{max} = M\left[(i_L R_L^U V_L^{-1}) + (i_H R_H^U V_H^{-1})\right] \tag{3}$$

$$I_L = \sum_{j=1,M} (i_L V_L^{-1} R_L) \tag{4}$$

$$I_H = \sum_{j=1,M} (i_H V_H^{-1} R_H) \tag{5}$$

$$G(\delta H_{FIN}) = 10^{-3}(H_M - H_m^{RULE})^2 (H^U - H^L)^{-2} \tag{6}$$

H_M is Gatun Lake level at the end of the M-month forecast horizon.
H_m^{RULE} is the rule curve value for calendar month m corresponding the end of the M-month forecast horizon.
H^U and H^L are Gatun Lake spill level and lowest level, respectively.

The evolution of Gatun Lake state (level, volume) is simulated as follows, where Q is a generic monthly inflow and R^* is the actual total release

$$\delta V = Q - E - R^* \tag{7}$$

where the total release R^* is comprised of the releases for lockage (R_L), hydropower generation (R_H), and spill (R_S):

$$R^* = (R_L + R_H + R_S) \tag{8}$$

with the volume conservation constraint describing the change from volume V_{t-1} to volume V_t,

$$V_t = V_{t-1} + \delta V \tag{9}$$

and with reservoir level (H_t) given as a function of volume

$$H_t = g(V_t). \tag{10}$$

In addition, any feasible policy is subject to the physical simulation of lake water budget (see below), including the lake level active storage constraint (11), and non-negativity and upper threshold constraints for releases:

$$H^L \leqslant H \leqslant H^U \tag{11}$$

$$0 \leqslant R_L \leqslant R_L^U \tag{12}$$

$$0 \leqslant R_H \leqslant R_H^U \tag{13}$$

$$0 \leqslant R_S \leqslant R_S^U \tag{14}$$

(Note: these constraints are generalized for simplicity above—further details are given in discussion of the "virtual manager" Section 2.4).

For this work, this problem is solved using the Simplex method [11] as implemented by [13]. To reduce the solution space for the optimization, the optimal policy is given in terms of a sequence of M total monthly releases (R^*), which are then allocated by a "virtual manager". The allocation of R^* is such that first priority is given to lockage, then to hydropower generation (with the constraint that hydropower production in the final month of the forecast horizon does not result in a lake level below the relevant rule curve value, H_m^*). Spillage is used only to bring the lake to a level just below H^U, except in the final month of the forecast horizon where, if possible, it is used to bring the lake level to H_m^*. Note that maximum spill capacities (R_S^U) are very large, so that management of spillage (and protection from damage from flooding) implicitly occurs on time scales finer than the monthly time steps of the

simulation procedure and is effective. Actual simulated spillage of excess volume did not approach full capacity, so simulated flooding did not occur.

2.3.2. Simulation procedure

This section describes the procedure through which the evolution of canal state is calculated given (A) the initial lake state, (B) relevant physical and economic invariants (both constants and functions), (C) a "virtual manager", and (D) a specified release policy. The simulation methodology used here is depicted schematically in the upper portion of Fig. 6 (see also Fig. 1). For the first simulated month (January, 1981), the initial lake volume (V_0) is set to the rule curve value for January 1 (H_1^*). For subsequent starts, V_0 comes from the assessment step for the preceding month (see Section 2.3.4 below). Given some current lake volume (V_t), monthly inflow and total release, the evolution of lake state is the simple budget calculation expressed by the Eqs. (7)–(10). The distribution of R^* among lockage, hydropower generation and spill is controlled by a "virtual manager". Some aspects of the behavior of the virtual manager have been noted already; for clarity they are formalized below.

At the beginning of a time step, the current lake volume, the forecast inflow, and uncontrolled losses (V_t, Q, and E) that will occur over the next time increment are known, so that, the available water supply and associated level are given by

$$V^1 = V_t + Q - E \tag{15}$$

with associated level

$$H^1 = g(V^1) \tag{16}$$

where above, and in the three steps below, the superscripted V (V^1, V^2, V^3) indicate volumes remaining after each budget computation. Given V^1, the total volume available at the beginning of the accounting, the virtual manager allocates lockage, hydropower and spillage in sequence as follows.

Step 1. Lockage

$$R_L = \max[\min(R_L^U, V^1 - V^L), 0] \tag{17}$$

$$V^2 = V^1 - R_L, \tag{18}$$

and

$$H^2 = g(V^2) \tag{19}$$

Step 2. Hydropower

If not at the end of the forecast horizon,

$$R_H = \max[\min(R_H^U, V^2 - V^L), 0] \tag{20}$$

otherwise,

$$R_H = \max[\min(R_H^U, V^2 - h(H_m^{RULE}), 0] \tag{21}$$

where the forecast horizon ends in month m.

$$V^3 = V^2 - R_H \tag{22}$$

$$H^3 = g(V^3) \tag{23}$$

Step 3. Spillage

If not at the end of the forecast horizon,

$$R_S = \max(0, V^3 - \delta_V) \tag{24}$$

$$\delta_V = h(H^U - \delta_H), \delta_H = 10\ \text{cm} \tag{25}$$

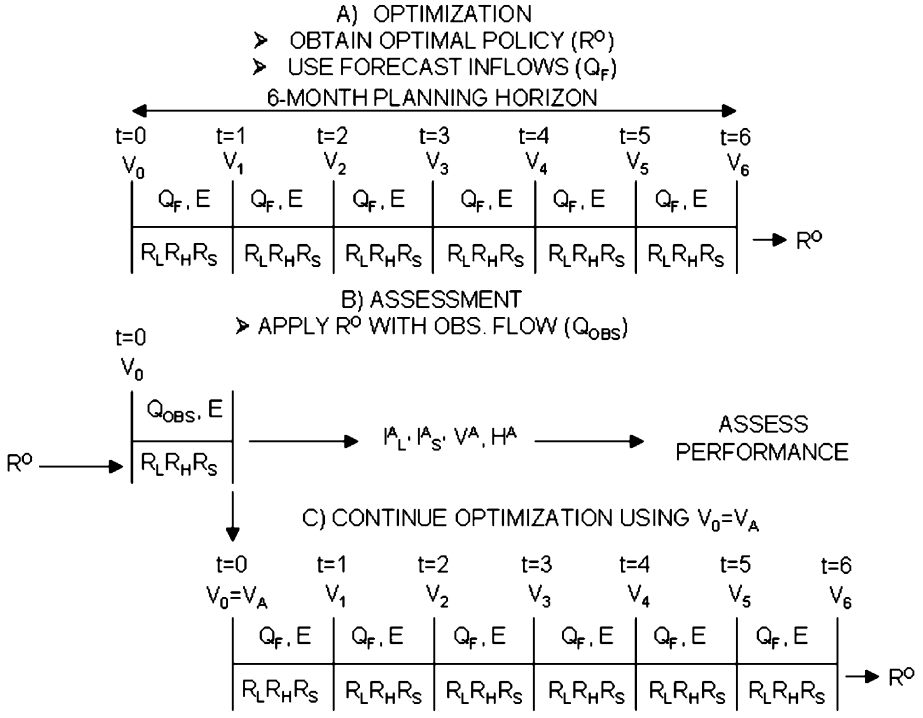

Fig. 6. Schematic of the optimization and assessment procedures.

otherwise

$$R_S = \max(0, V^3 - h(H_m^{RULE})) \quad (26)$$

$$V_{t+1} = (V^3 - R_S) = V_t + Q - E - R^* \quad (27)$$

and with R^* given by Eq. (8).

Terms required for evaluating the objective function are obtained from Steps 1 and 2 (see Eqs. (4) and (5)) and are summed monthly, and, at the end of the forecast horizon, the term signifying the departure of the lake level from the desired rule curve level is produced. Aside from tests for non-feasible solutions (e.g., negative or very large proposed releases), the procedure outlined above completely defines the simulator. The procedure was able to maintain the lake below H^U (flooding did not occur). Note that Step 3 formally invokes the idea that managed sub-monthly spillage will control lake level without resulting in economic loss, irrespective of the spill volume. Thus, for this "virtual manager", there is no risk associated with maintaining a high lake level.

2.3.3. Optimization

The Simplex procedure is initialized with a set of $M + 1$ candidate M-month release policies, each with an associated objective function value (R^C and J^C, respectively; not shown in Fig. 6). The $M + 1R^C$ are selected to sample locations near the boundary of the feasible solution space; the $M + 1$ associated J^C are obtained by applying R^C to the simulation system (described in the previous section) with the appropriate forecast inflow distribution (Q_F; i.e., the J^C are Monte Carlo sums across the forecast inflow distribution). The initial lake volume (V_0) for initialization comes from the volume obtained by applying the previous step's optimal solution for the first month of its forecast horizon using the observed flows for that month (i.e., this value of V_0, denoted V_0^A, comes from the assessment procedure, see Section 2.3.4).

It is important to recognize that (in every instance) a given objective function value represents the aggregate (e.g., summed) response of the system (i.e., the simulator) to a particular policy, under a particular initial state and forecast inflow distribution. It is through this process that probabilistic information concerning the potential gains and risks (costs and losses) associated with particular outcomes enters the solution.

Once initialized, the Simplex procedure seeks a minimum value of the objective function through an iterative process, moving through "policy space" as an $M + 1$ node polygon. Each candidate policy is evaluated in turn, and the distribution of the $M + 1$ values of J determines which node to move next and in which direction. Stopping criteria based on the number of "moves", or on the rate of change of the minimum J, terminate the search. A final perturbation to the node positions was used to ensure that the algorithm will not terminate at a local minimum.

Tests conducted using an exhaustive search procedure (with $M = 3$) showed that the Simplex method was relatively fast and accurate at finding minima. Not surprisingly, the tests also showed the solution space may have a complex topology, with many policies (sometimes well separated in solution space) having the same or similar values. Although this characteristic leaves the concept of a "best" solution ill-posed (and suggests the inclusion of other terms in the evaluation of J), it is at least a sensible portrayal of the hypothetical system. Further, extensive tests show that the solution procedure is robust in the sense that small perturbations in initial conditions yielded similar overall behavior in objective function values and assessed performance.

2.3.4. Assessment

The performance of the simulation/optimization system was assessed as shown in the middle portion of Fig. 6. Once an optimal policy has been selected, it is applied together with the appropriate initial volume (V_0) and the actual (observed) inflows to the first month of the forecast horizon. For the first month of the forecast sequence (January, 1981), V_0 was set to the January 1 rule curve value, and in subsequent months it is set to the volume at the end of the previous assessment step. Thus, the sequences of releases, incomes, and lake volumes/levels coming from the assessment portray the behavior of the system had the optimal release policies (generated using Q_F) been actually applied (i.e., Q_{OB} occurs).

2.4. Inflow forecasts

Three different sets of hypothetical inflow forecasts were used in the simulations. For one set, denoted CLIM (Q_F^{CLIM} where used symbolically), the forecast inflows were simply the observed monthly mean inflows ($\langle Q_{ob,m} \rangle$, i.e., climatology) for 1950–1980. Uncertainties in the CLIM inflow forecasts were cast in terms of the standard deviation of the historical inflows ($\sigma_{ob,m}$) for the month in question. Random inflow sequences (ensembles) were then generated using $\langle Q_{ob,m} \rangle$ and $\sigma_{ob,m}$. Restricting these random inflows to have positive values produced distributions in good agreement with actual distributions (note: the procedure does result in a very slight positive bias mean inflow of the Monte Carlo population compared with the original value).

Serial autocorrelation of the month-to-month inflows was considered in developing the methodology for deriving the CLIM forecast ensembles. The autocorrelations of observed inflow (1950–1999 data) range from relatively low values (0.05–0.4) during the wet season (boreal fall), with higher values during the boreal spring and early summer (0.4–0.7), with the maximum values for January–February and February–March. To get some sense of how much of this autocorrelation derived from the slowly varying impacts of El Niño variability, we calculated autocorrelations of residual inflows (i.e., the difference between observed inflows and those predicted on the basis of observed Niño3 SST (using linear regression, see below)).

The results show large reductions in month-to-month inflow autocorrelation during boreal spring/early summer suggesting that much of the autocorrelation during this season is due to ENSO-related precipitation variability rather than hydrologic processes (e.g., base flow). In any case, what the "climatological" forecasts represent ultimately depends on what assumptions a "virtual" inflow forecaster might make based solely on climatology. Further, adequately accounting for the hydrologic processes contributing to the autocorrelation would be problematic for the simple statistically-driven approach used here. For these reasons, we envisioned a "virtual" CLIM inflow forecaster who uses the simplest possible approach and bases the forecasts on long-term monthly means and variability.

A second set of inflow forecasts, denoted PERF, simulates those from a perfect forecast system—these flows follow the observed values with small uncertainties added (nominally $\sigma_{\mathrm{PERF}} = 0.01\sigma_{\mathrm{ob}}$). The same "positive-only" procedure discussed above was applied in generating the PERF forecasts. The third set of forecast inflows, denoted FCST, is intended to emulate flow forecasts that could be obtained using operationally available NINO3 data. In the first step, monthly regression coefficients were derived relating anomalies in monthly NINO3 SSTs to contemporaneous observed inflow over the period 1950–1980.

In the second step, these coefficients were applied to a set of retrospective and operational NINO3 forecasts produced by NCEP using the (now superseded) coupled forecast system described by [6,7]. These forecasts were initialized from assimilated oceanic conditions (see [8]) at monthly intervals from January, 1981 to December, 1997 and run out to a lead time of eleven months. The skill level of these forecasts is similar to that of other operational and experimental forecast models [9]. The correlations between observed and forecast NINO3 SST as a function of validation month and lead time are shown in Table 1. These correlations are very high at short lead times owing the fact that the model assimilates observed SSTs (and other oceanic data) as part of the initialization procedure. At longer lead times, correlations exceed persistence (e.g., [9]), and model skill is due largely to coupled dynamics. As is typical of such models, the forecast correlations in Table 1 tend to fall off with lead time more slowly during boreal winter and late fall than during summer. They show a tendency for forecasts to lose skill when their trajectories originate in, or cross, boreal spring [10,9].

The two-step procedure outlined above produced a set of forecast monthly inflows for the period January, 1981 (one-month lead time) through June, 1998 (six-month lead time). Uncertainties for these forecasts are stated in terms of the root-mean-square (RMS) errors between the forecast (Q_{FCST}) and observed (Q_{OBS}) inflows (see Table 2). These RMS errors are calculated as a function of forecast validation month and lead time and convolve uncertainties arising from (a) the relationship between observed inflows and NINO3 SST (Fig. 5), and (b) NINO3 forecast errors (Table 1). The degree to which the forecast inflows reduce uncertainty can be expressed as the ratio between the RMS errors for the FCST inflows to those for the CLIM forecasts (i.e., the standard deviations of the observed monthly inflows). These ratios are largest (i.e., little reduction in uncertainty compared with climatology) in forecasts for April to June, and for October, and smallest (greater reduction in uncertainty) in forecasts for August, September, November and December. For forecasts validating in these months, uncertainties are reduced by 15–25% compared with climatology at shorter lead times, with some tendency to decrease with lead time.

Table 1
Correlation (×100) between observed and forecast Niño3 SSTs 1981–1997

	1	2	3	4	5	6	7	8	9	10	11
1	98	96	98	95	86	86	73	81	52	54	33
2	98	94	94	92	92	79	83	72	81	63	41
3	96	90	94	94	85	79	76	82	74	83	67
4	92	89	84	81	73	73	54	48	64	71	68
5	96	86	83	81	70	62	34	64	40	47	72
6	96	89	91	76	77	61	49	24	72	19	36
7	97	93	78	80	65	60	60	53	26	52	27
8	97	92	90	77	71	71	41	71	48	19	55
9	97	86	82	85	65	49	75	37	65	32	9
10	98	91	78	80	87	60	58	76	29	63	34
11	99	97	89	85	84	88	56	63	55	34	55
12	99	98	94	86	82	78	85	57	65	47	36

Top row gives lead time months, left column gives validation month.

Table 2
Ratio (×100) of RMS inflow errors for estimates derived via regression from Niño3 SST forecasts with those from assuming climatological (long-term monthly mean) inflows

	1	2	3	4	5	6
1	92	94	93	93	95	96
2	89	81	85	83	81	91
3	88	90	89	89	90	86
4	100	100	100	97	95	96
5	99	99	99	99	99	99
6	103	97	101	97	103	97
7	83	84	82	86	90	100
8	75	75	70	75	78	76
9	94	96	94	94	96	100
10	99	99	97	97	98	96
11	83	85	83	80	85	78
12	76	78	77	85	88	84

Top row gives lead time months, left column gives validation month.

Ensembles of FCST inflow forecasts were generated in a similar manner to that used for the CLIM forecasts (see above), but in this case using the RMS flow errors as the basis for perturbing the forecast Niño3 SST regression-based estimates.

3. Results

Fig. 7 compares the performance of the PERF, CLIM, and FCST forecast sets in terms of total income (see Table 3 for parameter values). To explore the sensitivity of the

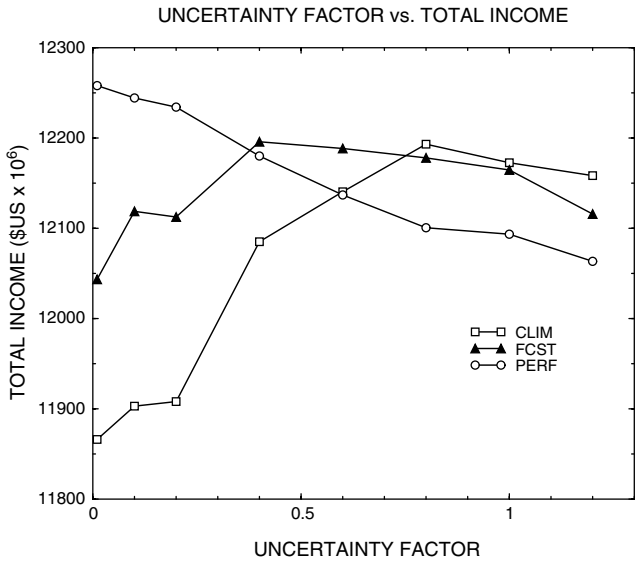

Fig. 7. Total simulated income (vertical axis; for the nominal (40 ships day^{-1}) case) vs. uncertainty factor (horizontal axis) for the CLIM (square), FCST (triangle), and PERF (circle) forecast sets.

different forecast sets to different levels of assumed uncertainty, integrations have been performed with each set allowing the uncertainties to range from 0.1 to 1.2 times their respective nominal values. As noted above, these are $1.00\sigma_{obs}$ (PERF, CLIM), and 1.00 $RMSE_F$ (FCST). As would be expected, the maximum value for the PERF forecasts of \$US 12.26×10^9 (the maximum possible income for the 204 assessment months is approximately \$US 12.40×10^9) is obtained using the lowest uncertainty (this is the total value for assessment month from the 204 forecast starts), and total income declines as uncertainty is increased. This downward trend with increasing uncertainty reflects the fact that the PERF forecasts are exactly correct; in such a case increased uncertainty reduces reliability, and the assumed optimal policies embody hedges against non-existent risks. It is also worth emphasizing that each of the curves in Fig. 7 has steep gradients over some range when considered a function of uncertainty. In that sense, accurately specified levels of uncertainty are critical.

The FCST forecasts behave differently from the PERF forecasts. In this case, the total value increases from approximately \$US 12.05×10^9 to \$US 12.19×10^9 with an uncertainty of about 40% of the nominal value, then decreases slowly. The initial increase in value with increasing uncertainty reflects the fact that these forecasts are not perfect. The fact that maximum income does not occur at the uncertainty-factor value of 1.0 where forecast reliability would be (at least approximately) maximized is mainly due to two reasons. First, the test period is relatively short and contains only two major El Niño episodes during which the simulated system was significantly stressed. For this reason, the behavior of the flow forecasts in a relatively few cases has a large effect on the outcome (i.e., the statistics are unstable). Second, in individual cases, the figure of merit used here (total income) may respond quite differently to forecast accuracy and uncertainty depending on current lake volume (lake state) and the actual flows experienced (the mapping of forecast accuracy to income is neither

Table 3
Parameters for simulated Panama Canal

Gatun Lake parameters
Useful volume (V^U)—766 Mm^3
Lowest useful level (H^L)—24.84 m
Maximum (spill) level (H^U)—26.67 m
Evaporation and municipal withdrawal (E) 6.16 Mm^3 month^{-1}
Maximum spill rate (R_S^U)—13358.30 Mm^3 month^{-1}
Actual spill rate per month (R_S) Mm^3
Rule curve level for a particular month (H_m^*) m
Actual level for a particular month (H_m^*) m
Canal parameters
Volume required per unit ship passage (V_L)—196,820 m^3 ship^{-1}
Maximum number of ships per month (S^U)—1200 ships month^{-1}
Maximum lockage volume per month (R_L^U)—236.18 Mm^3 month^{-1}
Actual lockage volume per month (R_L)
Volume required per unit MW h hydropower production (V_H)—19,114 m^3 MW h^{-1}
Maximum hydropower production per month—17,280 MW h
Maximum hydropower volume per month (R_H^U)—330.29 Mm^3 month^{-1}
Actual hydropower volume per month (R_H)
Income parameters
Income per ship passage (i_L)—\$US 50,000
Maximum lockage income per month (I_L^U)—\$US 60M
Actual lockage income per month (I_L)
Income per MW h (i_H)—\$US 50
Maximum hydropower income per month (I_H^U)—\$US 864,000
Actual hydropower production per month (I_H)
Maximum possible total income per month (I_{MAX})—\$US 60.864M

linear nor stationary). For example, very accurate forecasts of normal to high flows when lake level is relatively high do not produce much increase in income compared to somewhat less accurate forecasts because the perceived risks in either case are low and full lockage can be achieved with little added risk. The CLIM forecasts behave similarly to the FCST forecasts, but have lower total incomes for low assumed uncertainties, and peak at a higher uncertainty factor value. The maximum income for CLIM forecasts is slightly below the maximum value for the FCST set.

Fig. 8 compares net income over the 17 year assessment period for (A) the CLIM forecasts applied deterministically (uncertainty factor 0.01; essentially this assumes that climatological monthly mean inflows will occur every month), the PERF forecasts (uncertainty factor 0.01), and the FCST forecasts using the uncertainty factor of 0.4 (best overall performance for this set). For these assumptions, the use of flow forecasts derived from ENSO predictions produces an additional \$US 329×10^6 over the 17 year experiment, and increase of about 3% over that obtained using the CLIM forecasts. We note that this comparison would yield realistic results if the historical data were used to calibrate the uncertainty levels that produce maxima for the FCST and CLIM curves of Fig. 7.

To show the difference in behavior of the PERF (0.01 uncertainty factor) and FCST (0.40 uncertainty factor) Fig. 9 shows the time series of total monthly assessment month incomes for these simulations. It can be seen that in most years the simulated canal system is able to meet lockage demands (income is near the upper limit), and but that the reduced inflows during the 1997–1998 El Niño result in economic losses (curtailed lockage) in both simulations, and a large difference between the two. This is a general result when comparing the simulated results using the nominal demand levels described earlier with reasonable levels of uncertainty (and using observed inflows).

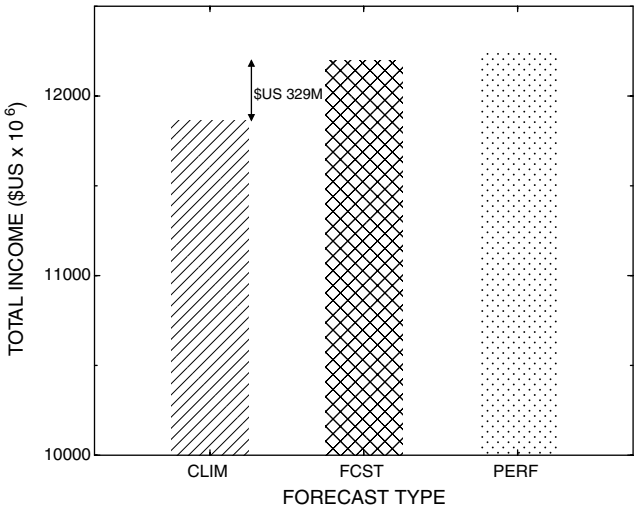

Fig. 8. Comparison of total income (vertical axis) for deterministic CLIM forecasts (uncertainty factor 0.01), probabilistic FCST forecasts (uncertainty factor 0.40), and deterministic PERF forecasts (uncertainty factor 0.01).

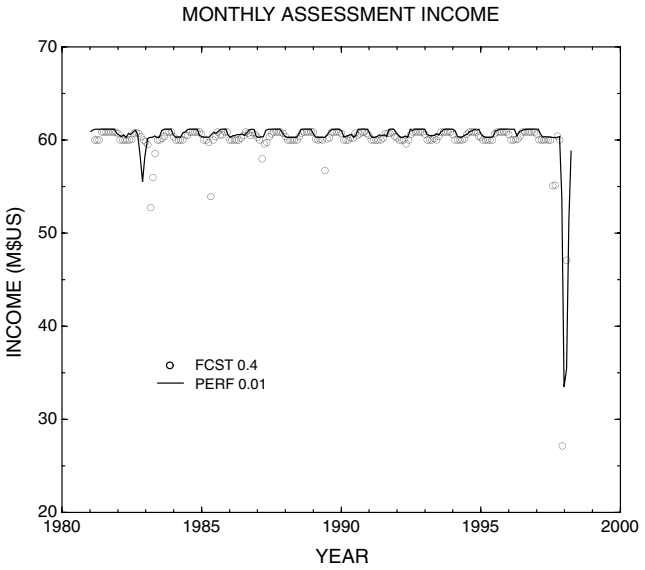

Fig. 9. Monthly incomes for the PERF (solid line) and FCST (open circles) forecasts.

Under these conditions, there is nearly always sufficient water to meet the demand for lockage (the dominating component of income), wet season inflow is generally sufficient to fill the Gatun Lake to capacity, and the 1997–1998 was so severe that even perfect foresight could not prevent losses.

Fig. 10 is similar to Fig. 7, but shows total income from hydroelectric generation for the three forecasts sets as a function of uncertainty level. In this case, the total income decreases rapidly with increasing uncertainty for each set. For the PERF forecasts at their maximum income uncertainty factor of 0.01 (from Fig. 8), the income is approximately \$US 94×10^6 over the forecast period. In comparison, the FCST forecasts produce \$US 81.5M at

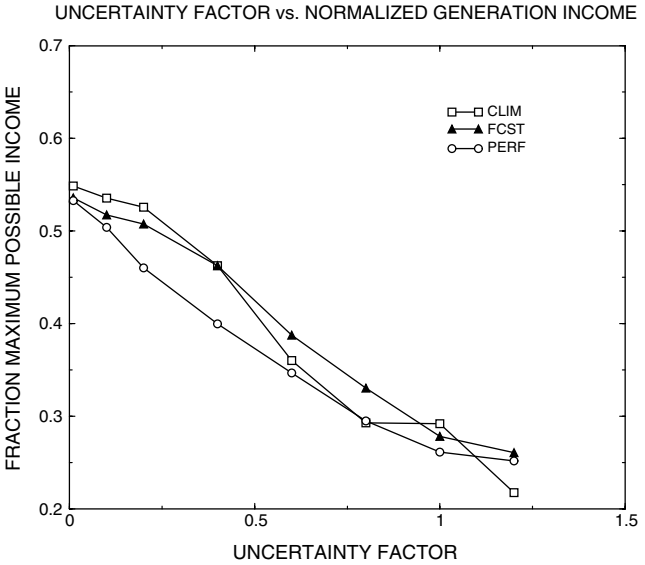

Fig. 10. As in Fig. 7, but for hydropower income (normalized by maximum possible hydropower income).

their maximum income point (uncertainty factor = 0.4), while the CLIM forecasts produce $US 51.6M at their maximum income location (uncertainty factor = 0.8). The high hydroelectric income for the low uncertainty factor FCST and the CLIM simulations reflects the fact that with small ensemble spreads (i.e., low uncertainty factors), there is (in general) little perceived risk and hence inappropriately high hydroelectric generation.

A point of interest regarding Fig. 10 is that the substantial difference between the FCST and CLIM hydropower income ($US 29.9M) is offset by an opposing difference in their lockage income at the maximum income point ($US 27.2M; $US 12114.2 M vs. $US 12141.4M, for FCST and CLIM, respectively), so that their net difference is just the $US 2.7M (both total and lockage incomes are shown in Fig. 7). It is possible that these differences are due to "noise" in the solutions (see Section 2) over the relatively short test period. However, it seems more likely that the differences reflect particular aspects of the FCST and CLIM inflow sequences (i.e., quality and timing of information) as they relate to the observed inflows. In this regard, note that (a) (except in 1997) simulated lockage deficits occurred only during the dry season when lake levels were especially low, and (b) lake levels are nearly always lower for the FCST (0.4 uncertainty factor) than for the more conservative CLIM (0.8 uncertainty factor) simulations. Thus it may be that the relative differences in lockage, hydropower, and total incomes in the FCST and CLIM simulations reflect (at least in part) different "rational" trade-offs between higher hydropower generation (and ensuing lower lake levels) vs. the risk of curtailed dry season lockage (except in 1997, simulated lockage deficits occurred only during the dry season when lake levels were especially low).

Fig. 11 corresponds to Fig. 10, but shows total spill as a function of uncertainty level. The behavior is the opposite from that for hydroelectric generation with the PERF, FCST and CLIM forecasts having increased spill as uncertainty level increases. For these assessment month simulations (with no direct negative impact on the objective function from spillage), spillage only occurs when lockage and hydropower generation allocations are maximized. At least to some degree, spillage represents unrealized past opportunities for hydropower generation when there was a perceived (but, in the end, incorrect) need to conserve water. The near perfect opposition of the hydropower and spillage curves results from this duality.

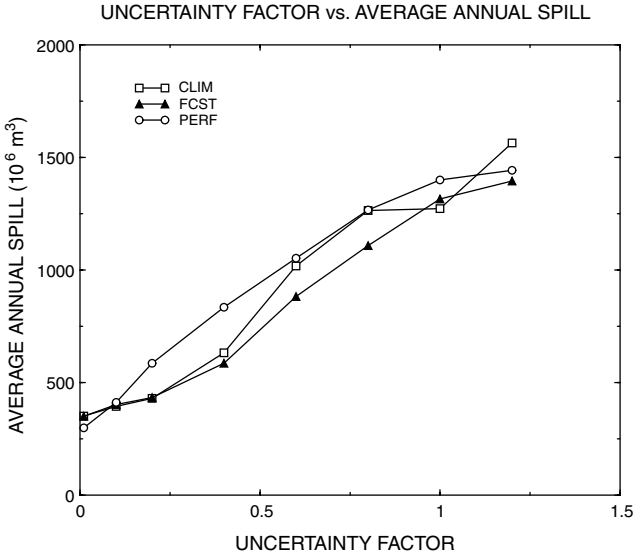

Fig. 11. As in Fig. 7, but for total annual spill.

The results in Table 2, Figs. 7 and 9 show the following points:

(A) FCST inflows possess some skill in that they have lower overall uncertainty than the CLIM inflows.
(B) Though perfect forecasts do add value (if they are known to be perfect), there is little separation between the CLIM and FCST results at their (simulation overall) optimal uncertainty levels.
(C) At optimal simulation levels, the simulated canal system was generally able to meet lockage demands and generate substantial hydropower using either the CLIM or FCST forecasts.

These points suggest that under the nominal demands and observed inflows the simulated canal system is not "stressed", i.e., Gatun Lake is sufficiently large and inflows sufficiently reliable that a large fraction of the total possible income can be produced by simply assuming climatological behavior (means and variability). In such a situation, forecasts would have to be quite skillful to produce increased value. We wondered how the relative value of the FCST data would change if the simulated system were subject to additional stress, and in the paragraphs below we examine the behavior of the simulated system when nominal lockage demand (R_L^U) increases by 20% and 40% (to 48 and 56 ships day^{-1}, respectively). This analysis is also pertinent to studying the canal watershed system ability to pass a larger number of ships than present if operational lockage capacity is increased.

Fig. 12 compares the total income (lockage + hydropower) from three sets of simulations using nominal lockage demands of 40 (same data as Fig. 7), 48 and 56 ships day^{-1}, here expressed as normalized income (fraction of total possible income for the nominal lockage demand). One of the results is that even with perfect forecasts the simulated canal system falls from 99% of total possible income for 40 ships to 97% and 93% for lockage demands of 48 and 56 ships, respectively (normalized lockage incomes (not shown) are 99%, 97%, and 94%, respectively)). A number of other points of interest from Fig. 12 are highlighted below:

- All the curves in Fig. 12 become steeper with respect to uncertainty as demand increases and uncertainty levels increase beyond the maximum income point. Thus, as the simulated canal system is increasingly stressed,

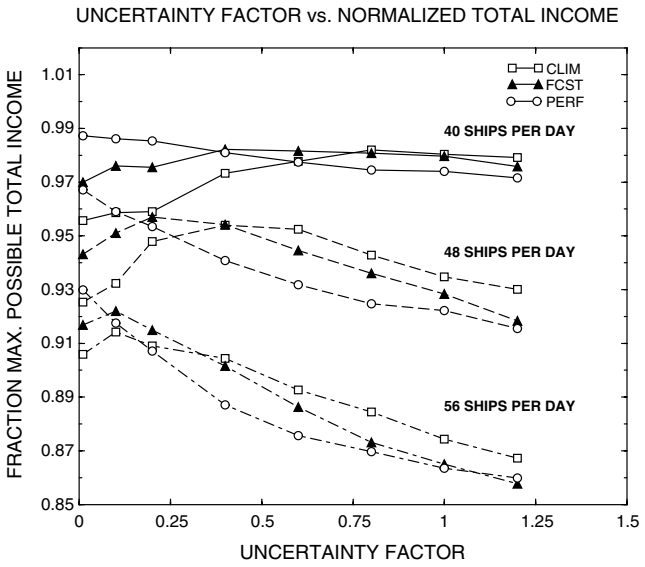

Fig. 12. Fraction of total possible income(lockage + hydropower) for simulations with maximum lockage set to 40 ships day^{-1} (solid curves), 48 ships day^{-1} (dashed curves), and 56 ships day^{-1} (long-short dashed curves). CLIM, FCST and PERF results are indicated with squares, triangles and circles, respectively.

correct specification of uncertainty level becomes more important. In this case the stress is applied by higher demand, but decreased inflows or storage capacity would have similar effects.

- The difference in fractional total income between deterministic perfect and climatology forecasts (PERF.0.01 and CLIM.0.01) is largest for the 48 ship case (the difference is largest in terms of actual income as well). The much smaller difference for these forecasts for the 56 ship experiments indicates that at this level of demand the canal system is stressed to the degree that forecast information is of less value (inflows are insufficient for operations in any case, and large losses ensue).
- The peaks of the CLIM and FCST curves move towards decreased uncertainty (to the left) as demand is increased. This behavior may be attributed to the fact that, as demands increase, the number of instances in which management can make a difference decreases (in other cases, lockage (and canal system behavior in general) is enforced by lake level, not management). The optimal level of uncertainty as far as canal management is concerned is thus smaller being associated with a small number of particular cases (presumably with high inflows) where decisions can affect the outcome.
- Finally, as surmised above, difference between the maximum relative incomes obtained using the FCST instead of CLIM forecasts does increase as demand is increased.

4. Summary and concluding discussion

An operations model has been used to investigate the economic value of seasonal El Niño forecasts for the Panama Canal, and to consider in a broader context the response of water resources systems to probabilistic inflow forecasts. The Panama Canal offers an interesting setting for such a study for several reasons. First, the Canal relies on precipitation for its water supply, and rainfall in the region is strongly modulated by tropical Pacific SSTs. Second, the Canal (at least as simulated) is physically straightforward and management goals are simple to state. Third, Canal operations and income are impacted during severe El Niño episodes.

Three types of forecasts were used, PERF (perfect) in which the mean of the forecast ensemble agreed with observations, CLIM (climatology), in which the central tendency of the forecast ensemble is the long-term monthly mean, and FCST (operational forecasts), in which the mean of the inflow forecasts was derived from operational forecasts of tropical Pacific SSTs.

The modeling system is made up of three components—a simulator/virtual manager, an optimizer, and an assessment module. The simulator/virtual manager embodies the physical characteristics of Gatun Lake including capacity, critical volumes and levels volume-to-level relationships, lockage, hydropower and spill constraints, and some basic guidelines concerning canal operations. Given an initial Gatun Lake volume, a projected inflow sequence, and a release policy for a one-month time step, the simulator/virtual manager implements releases for lockage, hydropower and spill. Each of these alters Lake volume and the former two produce income.

The optimizer works in the context of a specified initial volume and a prescribed ensemble of forecast monthly inflows covering the six-month planning horizon. Given these data, the optimizer seeks a sequence of six monthly releases (the release policy) that it minimizes the expected value of a defined objective function. For our simulations, the objective function is driven principally by income, with an additional contribution from Lake level at the end of the planning horizon.

The assessment module then applies the selected optimal release policy for the first month of the planning horizon to the simulator, using the same initial volume prescribed the optimizer, and the observed inflow for that month. The behavior of the Canal system in these assessment steps (e.g., lockage and hydroelectric income, Lake level), allows quantification of the performance of the full system with a given set of forecast data. The Lake volume at the end of each assessment step provides the initial volume for the following optimization and assessment steps.

The simulated Canal system differs in a number of respects from the real one. Perhaps most importantly, the simulated system does not contain Madden Lake which has an active storage volume about 85% that of Gatun Lake and provides added storage to the system. Also, the simulated system does not have a formal demand for municipal water supply, which represents 6% of the total water usage for the actual system. Another major difference is resolution of the time step; water supply for the actual Canal system is managed at daily or finer time steps, so

aspects of policy development are different, and a finer balance between inflows and releases can be maintained. Also, at these finer time steps high rates of spillage can have some negative impact on operations, an effect that was not included in our system. Despite these approximations, the simulated system emulates many important attributes of the real system, the forcing functions (inflows) are realistic, and the assessment procedure shows how such a system would behave given various sorts of forecast information.

The results show that with current demands, and in the present climatological setting, the simulated Canal system is relatively resistant (in terms of meeting lockage demands) to all but the more extreme instances of inflow deficits. Contributing to this resistance is the practical limit on lockage and the fact that wet season inflows are nearly always sufficient to erase past deficits. The results also emphasize the following key points:

(1) An accurate measure of uncertainty is critical. Deterministic climatological forecasts performed very badly, but forecasts with the correct central tendency and a climatological estimate of uncertainty fared poorly as well. In this sense, characterization of forecast uncertainty can be as important as forecast accuracy.
(2) Despite the fact that ENSO forecast-derived inflow projections (FCST) are less uncertain that those derived from climatology (CLIM), they produce a rather small increase in total income under current demands. This is partly because in most years there is relatively little risk to income if hydroelectric generation is managed conservatively, and the FCST forecasts do not have sufficient discrimination to work at the margins much better than the CLIM forecasts. At the other extreme, during the 1997–1998 El Niño inflows were diminished to the point where the simulated system was unable to cope even with perfect foreknowledge. It is between these two extremes of very low risk and extreme stress that forecasts can provide value.
(3) The value of seasonal climate forecast information increased relative to climatology as demands on the simulated Canal system were increased. However, these increases were not large, and for substantial demand increases the Canal's ability to meet demands 100% of the time was compromised.

A useful extension of this work would be the incorporation of finer resolution operations (down to the daily level) in conjunction with the commensurate more detailed modeling of the physical canal system (e.g., including Lake Madden). The ideas in [4] using an end-to-end integrated forecast-management system and the existing Panama Canal watershed hydrometeorological forecast system [5] could provide the basis for such an extension. With these methodologies and tools, and following the approach described in the present paper, planning questions of potential system performance under canal capacity expansions and possible climatic change may be reliably addressed and answered.

Acknowledgments

The research work was sponsored by the NOAA Office of Global Programs under Grant No. DG133R-02-SE-0775. Additional support was provided by the Autoridad del Canal de Panama for the work of Carlos Vargas and Modesto Echevers. The ideas and opinions expressed in the paper are those of the authors and need not reflect those of the funding agencies and their sub-agencies.

References

[1] Dononso M, Vargas C, Castillero M, Martinez D, Leaman K, Nakayama M. Panama Canal case study. In: Glantz MH, editor. Once burned, twice shy: lessons learned from the 1997–1998 El Niño. Tokyo: United Nations University Press; 2001. p. 294.
[2] Enfield DB, Alfaro EJ. The dependence of Caribbean rainfall on the interaction of the tropical Atlantic and Pacific oceans. J Climate 1999;12:2093–103.
[3] Estoque MA, Luque J, Chandeck-Montzea M, Garcia J. Effects of El Niño on Panama rainfall. Geofis Int 1985;24:355–81.
[4] Georgakakos KP, Graham NE, Carpenter TM, Georgakakos AP, Yao H. Forecasts and multiobjective reservoir management in Northern California. EOS 2005;86(12):122. 127.
[5] Georgakakos KP, Sperfslage JA. Operational rainfall and flow forecasting for the Panama Canal watershed. In: Harmon RS, editor. Rio Charges, a multidisciplinary profile of a tropical watershed. New York: Springer; 2005. p. 354 [chapter 22].
[6] Ji M, Kumar A, Leetmaa A. A multiseason climate forecast system at the National Meteorological Center. Bull Am Meteorol Soc 1994;75:569–77.
[7] Ji M, Kumar A, Leetmaa A. An experimental coupled forecast system at the National Meteorological Center: some early results. Tellus 1994;46A:398–418.
[8] Ji M, Leetmaa A, Derber J. An ocean analysis system for seasonal to interannual climate studies. Mon Weather Rev 1995;123:460–81.
[9] Kirtman BP, Shukla J, Balmaseda, M, Graham, N, Penland C, Xue Y, et al. Current status of ENSO forecast skill. A report to the Climate Variability and Predictability (CLIVAR) Numerical Experimentation Group (NEG), CLIVAR Working Group on Seasonal to Interannual Prediction, 2002. Available from: http://www.clivar.org/publications/wg_reports/wgsip/nino3/report.htm.
[10] Latif M, Graham NE. How much predictive skill is contained in the thermal structure of an OGCM? J Phys Oceanogr 1992;22:951–62.
[11] Nelder JA, Mead R. A simplex method for function minimization. Comput J 1965;7:308–13.
[12] Panama Canal Authority, 2003. 2003 Annual Report. Available from: www.pancanal.com/eng/general/reporte-anual/index.html [accessed May 11, 2005].
[13] Press WH, Flannery BP, Teukolsky SA, Vetterling WT. Numerical recipes: the art of scientific computing. Cambridge UK: Cambridge University Press; 1992. p. 408–12.
[14] Reynolds RW, Smith TM. Improved global sea surface temperature analyses using optimum interpolation. J Climate 1994;7:929–48.
[15] Ropelewski CF, Halpert MS. Global and regional scale precipitation patterns associated with the El Niño/Southern Oscillation. Mon Weather Rev 1987;115:1606–26.
[16] Smith TM, Reynolds RW. Extended reconstruction of global sea surface temperatures based on COADS data (1854–1997). J Climate 2003;16:1495–510.
[17] World Bank, 2005. Available from: www.worldbank.org/data/databytopic/GDP.pdf [accessed May 11, 2005].